Oscillations in the Concentration of Fluoride Ions Induced by a pH Oscillator

Viktor Horváth,[†] Krisztina Kurin-Csörgei,[†] Irving R. Epstein,*[,‡] and Miklós Orbán*[,†]

Department of Analytical Chemistry, L. Eötvös University, H-1518 Budapest 112, P.O. Box 32, Hungary, and Department of Chemistry and Volen Center for Complex Systems, MS 015, Brandeis University, Waltham, Massachusetts 02454-9110

Received: December 3, 2007; In Final Form: February 7, 2008

Sustained oscillations in the concentration of free fluoride ions can be generated when the $BrO_3^--SO_3^{2-}-$Mn(II) oscillator is coupled either to $Al^{3+}-F^-$ complex formation or to the $Ca^{2+}-F^-$ precipitation process in a flow reactor. By careful analysis of the relevant equilibria and optimization of the reactant concentrations, one can obtain $[F^-]$ oscillations of several orders of magnitude as measured with an ion-selective electrode. The $BrO_3^--SO_3^{2-}-$Mn(II)$-Al(NO_3)_3-$NaF system also exhibits bistability, that is, simultaneously stable steady states of high and low $[F^-]$.

Introduction

In the vast majority of oscillatory chemical systems discovered to date, the positive feedback process, an essential component of the periodic behavior, is based on redox chemistry. From this observation, one might be tempted to draw the false conclusion that elements that do not possess multiple oxidation states are unable to participate in temporally or spatially periodic chemical processes. Recent studies,[1,2] however, have shown that periodic increases and decreases in the concentrations of ions and compounds of such elements can be induced by a redox-based primary or core oscillator when it is coupled to a complexation or precipitation equilibrium in which the target species are incorporated. Under some special conditions,[2] a key intermediate of the redox oscillator is able to drive the system between the reactant- and the product-dominated states of the equilibrium, and all participants in the total system undergo periodic concentration variations with the frequency of the core oscillator.

Using a design method suggested in ref 1, we were able to produce periodic pulses in the concentration of free calcium ions[2] when the $BrO_3^--SO_3^{2-}-Fe(CN)_6^{4-}$ pH oscillator[3] (abbreviated as BSF)[4] was used to force the pH-sensitive $Ca^{2+}-$EDTA reaction. Our aim is to involve more single-oxidation-state elements in periodic chemical phenomena. Here, we demonstrate that sustained oscillations in $[F^-]$ can be generated when the $BrO_3^--SO_3^{2-}-$Mn(II) oscillator is coupled either to the $Al^{3+}-F^-$ complex formation reaction or to the $Ca^{2+}-F^-$ precipitation process.

Experimental Section

Chemicals and Apparatus. The following chemicals were used: $NaBrO_3$ (Fisher), Na_2SO_3 (A.C.S Reagent Aldrich), $Mn(ClO_4)_2\cdot 6H_2O$ (Friedrick Smith Chem. Co.), $MnSO_4\cdot H_2O$ (Reanal), $Al(NO_3)_3\cdot 9H_2O$ (Fisher), $CaNa_2$EDTA (ethylenediaminetetraacetic acid calcium disodium salt hydrate 98%, Aldrich), and $HClO_4$ (Carlo Elba).

The reactions were carried out and monitored in a thermally regulated flow reactor (CSTR) of volume 35.0 cm^3, operated at 45 °C. The experimental setup is shown in Figure 1. The reactor was fed through four input tubes by a Gilson Miniplus 2 peristaltic pump. Mixing of the reactor contents was accomplished with a magnetic stirrer at a constant stirring rate of 600 rpm. Excess solution was continuously removed from the reactor via an outlet tube of larger internal diameter connected to another pump rotated in the opposite direction. The concentrations of the stock solutions prepared for generation of high-amplitude pH oscillations in the CSTR were $[NaBrO_3]_0 = 0.6$ M, $[Na_2SO_3]_0 = 0.472$ M, $[MnSO_4]_0 = 0.009$ M, and $[HClO_4]_0 = 0.0551$ M. All solutions but Na_2SO_3, which must be freshly made and used within 3−4 h, can be stored for an indefinite time. The concentrations of the reagents in the CSTR after mixing (before any reaction took place) were fourfold lower. We refer to this system as the "standard composition" of the $BrO_3^--SO_3^{2-}-$Mn(II) pH oscillator.[5] The changes in pH and in $[F^-]$ and $[Ca^{2+}]$ during the CSTR experiments were monitored with a combination glass electrode (Radelkis OP− 0823P), a combination F^- ISE (Thermo-Orion 9809 BNWP), and a combination Ca^{2+} ISE (Orion 93-20), respectively. The data were recorded on a PC using a pH meter (Radelkis OP208/1), a 16-bit multichannel digital−analog converter (NI-6010 PCI), and a multichannel recorder (Kipp & Zonen BD-51).

Selection of the Subsystems. In order to induce oscillations in $[F^-]$, we identified fast equilibrium reactions involving F^- ions and coupled these to a core system that produces the oscillatory dynamics. For the core oscillator, we selected the $BrO_3^--SO_3^{2-}-$Mn(II) CSTR system.[5] This system (abbreviated as BSM) at the standard composition showed oscillations in pH between 2.5 and 7.2 with a period of 24 min at $t = 45$ °C and flow rate $(k_0) = 3.7 \times 10^{-3}$ s^{-1} (residence time 4.55 min). Typical oscillatory traces are shown in Figure 2. In order to design oscillations in $[F^-]$, we first constructed an "Al oscillator" or a "Ca oscillator" by connecting the pH-sensitive hydrolysis reaction of Al^{3+} (eq 1) or the pH-dependent dissociation and formation of the CaEDTA complex (eq 2) to the core pH oscillator

$$Al^{3+} + 3H_2O \equiv Al(OH)_3 + 3H^+ \qquad (1)$$

* To whom correspondence should be addressed. E-mail: epstein@brandeis.edu (I.R.E.); orbanm@ludens.elte.hu (M.O.).
† L. Eötvös University.
‡ Brandeis University.

10.1021/jp7114115 CCC: $40.75
Published on Web 05/01/2008

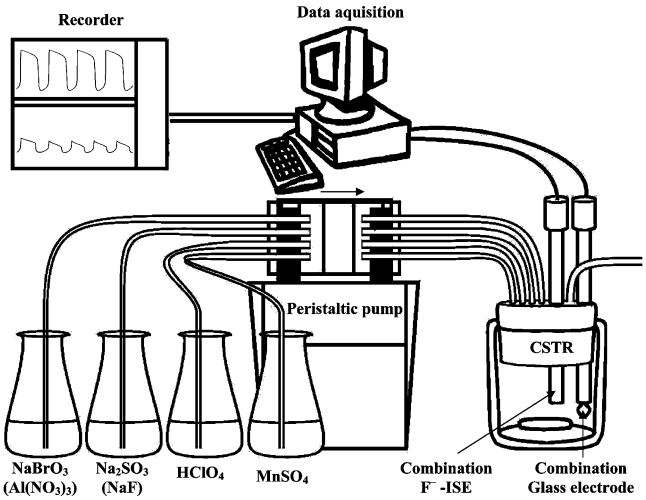

Figure 1. Experimental setup.

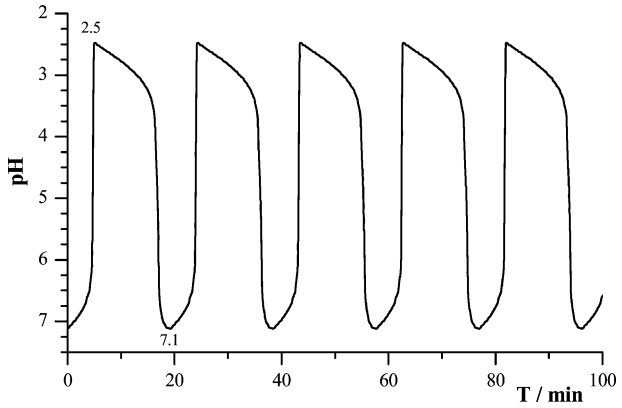

Figure 2. Oscillations in pH measured in the BSM oscillator. Initial concentrations in the CSTR (if no reaction took place) are $[NaBrO_3] = 0.15$ M, $[Na_2SO_3] = 0.118$ M, $[MnSO_4] = 2.25 \times 10^{-3}$ M, and $[HClO_4] = 1.38 \times 10^{-2}$ M; the temperature is 45 °C; the flow rate (k_0) is 3.7×10^{-3} s^{-1}; and the stirring rate is 600 rpm.

$$CaEDTA^{2-} \equiv Ca^{2+} + EDTA^{4-} \quad (2)$$

The BSM core oscillator drives the reactions in eqs 1 and 2 back and forth and provides high and low concentrations of free Al^{3+} or Ca^{2+} ions. When we introduce F^- ions into the BSM−$Al(NO_3)_3$ or the BSM−CaEDTA subsystems, new equilibria are established. The hard Lewis base F^- is known to form a stable complex or a sparingly soluble precipitate with the hard Lewis acids Al^{3+} and Ca^{2+} according to eqs 3 and 4

$$Al^{3+} + nF^- \equiv AlF_n^{(n-3)-} \quad (3)$$

$$Ca^{2+} + 2F^- \equiv CaF_2 \quad (4)$$

where $n = 1-6$. The log K_n (stepwise formation constants of the Al^{3+}−F^- complexes) are 6.1, 5.0, 3.8, 2.7, 1.6, and 0.5, and log K_{sp} (solubility product of CaF_2) = −10.41. Due to the cross-talk between the core oscillator and the equilibria in eqs 1−4, pH-induced oscillations in the concentrations of Al^{3+}, Ca^{2+}, as well as in $[F^-]$ may be expected to occur in the BSM−$Al(NO_3)_3$−NaF and BSM−CaEDTA−NaF systems.

Responses of F^- ISE to $[F^-]$, to pH, and to the Components of the pH Oscillator. The potential of the F^- ISE measured in a reaction mixture depends on a number of factors. The F^- ISE responds first of all to changes in $[F^-]$, but it is also sensitive to the pH and to the ionic strength. When the F^- ISE is used to follow $[F^-]$ in the BSM−$Al(NO_3)_3$−NaF system, quantitative measurement of $[F^-]$ cannot be achieved because not only $[F^-]$ but also the pH and the composition undergo changes during the oscillatory cycle. While we may not be able to determine $[F^-]$ exactly with our F^- ISE, we can estimate the relative changes in $[F^-]$ from its potential recorded in time. The F^- ISE used in our experiments showed Nernstian response to the changes in $[F^-]$. The potentials measured in distilled water at $[F^-] = 10^{-1}-10^{-5}$ M span from −100 to +140 mV. The relationship between the measured potential (in mV) versus $[F^-]$ was found to be $E = -178-60.5 \log[F^-]$. We also measured the potential versus $[F^-]$ curves at pH 4.0, 3.0, and 2.2. When we lowered the pH, the potential of the F^- ISE shifted toward higher values by 5−30 mV (depending on the pH), but we observed no noticeable change in the slope. When no F^- ions were present, the F^- ISE showed an uncertain high potential (>200 mV) in distilled water, which further increased to about 360 mV as we decreased the pH to 2. We tested the response of the F^- ISE in the standard composition oscillatory BSM system in the presence and in the absence of F^-. Without F^-, when the pH oscillated between 7.2 and 2.5, the F^- ISE showed oscillatory potentials between 270 and 370 mV, with a sharp peak of 440 mV when the pH abruptly jumped from 7.2 to 2.5. These potentials fall outside of the range of values shown by the F^- ISE at any pH when it functions as a F^- ion sensor in a F^--containing environment. When we introduced $[F^-] = 6.25 \times 10^{-4}-2.5 \times 10^{-3}$ M (the concentrations used in our CSTR experiments), the potential shifted back to the normal values. In the BSM−NaF system, in addition to the pH oscillations, the F^- ISE signal also oscillated in time, despite the lack of any direct interaction between F^- and the components of the pH oscillator. These oscillations, which result from the protonation of F^- to form HF (pK = 3.14) at the lower end of the oscillatory pH range, do not exceed 30−40 mV. From these findings, we conclude that if the amplitude of oscillations measured with the F^- ISE in the BSM−$Al(NO_3)_3$−NaF or BSM−CaEDTA−NaF systems at $[NaF] = 6.25 \times 10^{-4}-2.5 \times 10^{-3}$ M is larger than 30−40 mV, the difference may safely be attributed to oscillations in $[F^-]$ induced by pH changes in the total system. The "matrix effect", that is, the effect of components other than NaF on the potential of the F^- ISE, also produces some shift in the oscillatory traces toward higher potential.

Results and Discussion

Construction of an "Al Oscillator". For generating periodic fluxes in $[Al^{3+}]$, we coupled the pH oscillations depicted in Figure 2 to the hydrolysis of Al^{3+} (eq 1). We introduced Al^{3+} into the standard-composition BrO_3^-−SO_3^{2-}−Mn(II) oscillatory system by mixing $Al(NO_3)_3$ with the input $NaBrO_3$ solution, making the total concentration of the Al salt in the CSTR 6.25×10^{-4} M. The $[Al(NO_3)_3]$ ($\leq 6.25 \times 10^{-4}$ M) had only a minimal effect on the range of pHs in which the oscillator operated. However, as we increased $[Al(NO_3)_3]$ further, the time the pH oscillator spent in the acid range grew. At $[Al(NO_3)_3] \geq 2.5 \times 10^{-3}$ M, the oscillations terminated, and the system maintained a steady pH of around 3−4.

During the oscillatory cycle, dramatic visual changes occurred in the reactor. The reaction mixture was crystal clear at low pH. At pH 3.8, turbidity started to appear, and the reactor filled with white precipitate above pH 4.5.

For identification of the Al species in the clear and cloudy states, we calculated the distribution of Al species in a 6.25×10^{-4} M $Al(NO_3)_3$ solution (the concentration used in the

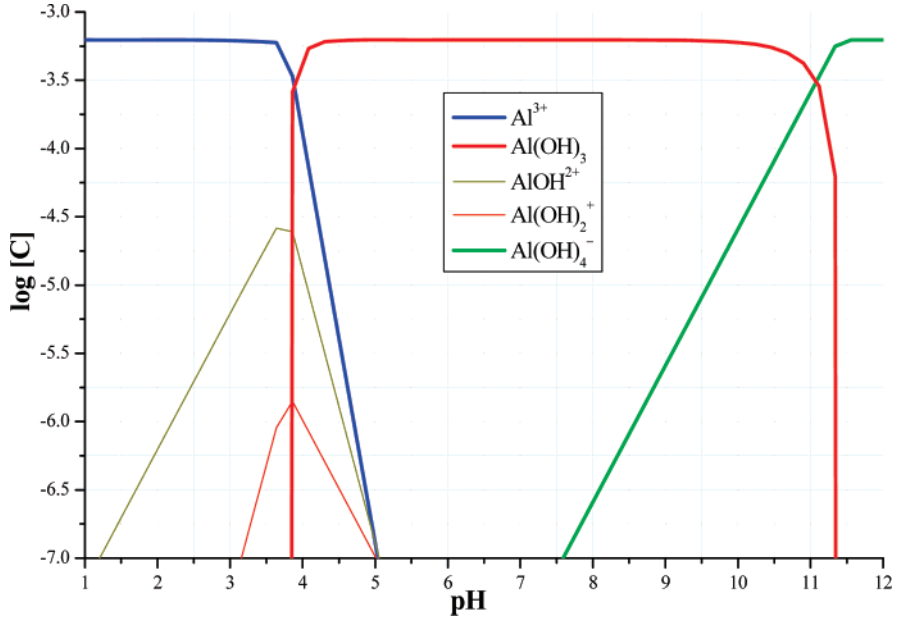

Figure 3. Distribution of species in the $[Al(NO_3)_3] = 6.25 \times 10^{-4}$ M solution as a function of pH.

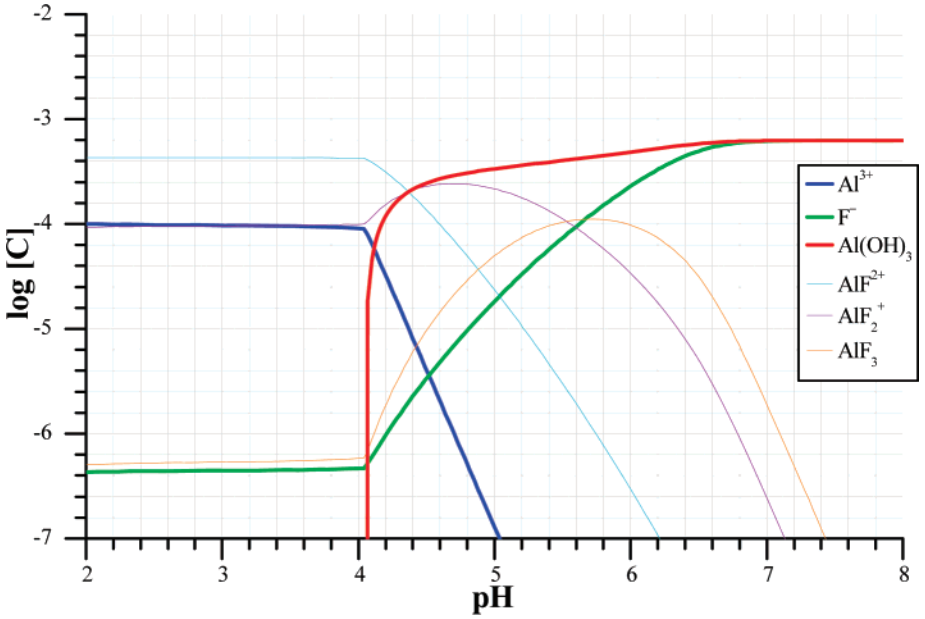

Figure 4. Distribution of species in a mixture containing $[Al(NO_3)_3] = [NaF] = 6.25 \times 10^{-4}$ M as a function of pH.

oscillatory mixture) as a function of pH using the program MEDUSA.[6] The results are shown in Figure 3. The diagram supports the expectation that at pH < 3.8, all of the aluminum is present as free Al^{3+}; at pH > 3.8, it is precipitated in the form of $Al(OH)_3$. The periodic appearance and dissolution of the white precipitate indicate the existence of high-amplitude periodic pulses in the free $[Al^{3+}]$ induced by the changes of pH in the BSM−$Al(NO_3)_3$ subsystem.

Design of a F^- Oscillator. *Oscillations in $[F^-]$ in the BSM−$Al(NO_3)_3$−NaF System.* In order to design a F^- oscillator, we employed the following working hypothesis. When F^- ions are introduced into the "Al oscillator", in addition to the hydrolysis reaction of Al^{3+}, a second equilibrium, complex formation between Al^{3+} and F^-, takes place according to eq 3. The equilibria in eqs 1 and 3 are coupled through the free $[Al^{3+}]$. The extent of the reaction in eq 1 is directly and the reaction in eq 3 is indirectly influenced by the BSM oscillator. As a result, under proper conditions, oscillations in $[F^-]$ can occur in the BSM−$Al(NO_3)_3$−NaF flow system.

In order to find the optimum concentrations to be used in the combined system for obtaining high-amplitude oscillations in $[F^-]$, we calculated with MEDUSA the distribution of all species present in the $Al(NO_3)_3$−NaF subsystem as a function of pH. We performed calculations with $[Al(NO_3)_3] = 6.25 \times 10^{-4}$ M and $[NaF] = 6.25 \times 10^{-4}$, 1.25×10^{-3}, 2.5×10^{-3}, and 3.75×10^{-3} M, corresponding to initial $[Al^{3+}]/[F^-]$ ratios of 1:1, 1:2. 1:4, and 1:6, respectively. These diagrams allowed us to estimate the concentration of free F^- ions and those of all species in which fluoride is bound to H^+ or Al^{3+}, that is, HF, AlF^{2+}, AlF_2^+, AlF_3, AlF_4^-, AlF_5^{2-}, and AlF_6^{3-}, as the pH was varied between 2 and 8. As an example, the diagram calculated at $[Al(NO_3)_3] = [NaF] = 6.25 \times 10^{-4}$ M is presented in Figure 4, and a more detailed plot is given in the Supporting Information. The calculations show that the $[F^-]$ is high at high

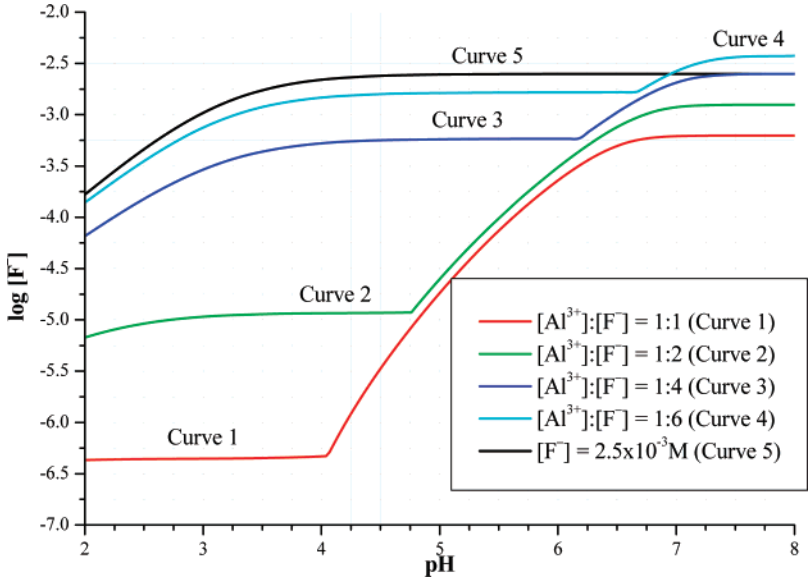

Figure 5. Calculated concentration of free [F⁻] as a function of pH in mixtures with constant [Al(NO$_3$)$_3$] = 6.25 × 10^{-4} M and increasing [NaF] = 6.25 × 10^{-4} (curve 1), 1.25 × 10^{-3} (curve 2), 2.5 × 10^{-3} (curve 3), 3.75 × 10^{-3} M (curve 4), and 2.5 × 10^{-3} M solution (curve 5).

pHs but low at low pHs. The dominant complex species formed in the Al(NO$_3$)$_3$−NaF system in the low pH range are AlF^{2+} (and AlF_2^+) at 1:1, AlF_2^+ (and AlF^{2+}) at 1:2, AlF_3 (and AlF_2^+) at 1:4, and AlF_3 (and AlF_4^-) at 1:6 ratios of [Al(NO$_3$)$_3$]$_0$ to [NaF]$_0$.

From the [species] versus pH diagrams, we extracted the free [F⁻] versus pH plot for each composition, as shown in Figure 5, curves 1−5. Curves 1−4 represent [F⁻] at constant [Al(NO$_3$)$_3$] = 6.25 × 10^{-4} M and increasing [NaF] = 6.25 × 10^{-4} (1:1), 1.25 × 10^{-3} (1:2), 2.5 × 10^{-3} (1:4), and 3.75 × 10^{-3} M (1:6). Curve 5 is [F⁻] versus pH at [NaF] = 2.5 × 10^{-3} M without Al(NO$_3$)$_3$.

From curves 1−5 of Figure 5, we can draw the following conclusions:

(1) When F⁻ and Al^{3+} are combined in different molar ratios and the pH changes from 2 to 8 (curves 1−4), the largest change in the free [F⁻] (about 3 orders of magnitude) appears if the initial ratio of [Al(NO$_3$)$_3$] to [NaF] is 1:1. If the ratio increases, the change decreases; it is 2 orders of magnitude at 1:2, 1.5 at 1:4, and about 1 order of magnitude at 1:6.

(2) Comparison of the log[F⁻] values at the two ends of curves 1−4 reveals—as can be more clearly seen from the [species] versus pH diagrams in the Supporting Information—that at pH 2−3, essentially all of the fluoride is complexed. As the pH increases, OH^- successfully competes with F⁻ for Al^{3+}, and Al(OH)$_3$ starts to precipitate. In the absence of F⁻, this occurs at pH 3.8 (see Figure 3). If F⁻ is also present, this pH shifts toward higher values. The break points on curves 1−4 represent the initial pH of precipitation at [Al(NO$_3$)$_3$]$_0$/[NaF]$_0$ = 1:1, 1:2, 1:4, and 1:6, where these pHs are 4.1, 4.8, 6.2, and 6.6, respectively. Displacement of the F⁻ ligand from the complex $AlF_n^{(n-3)-}$ by OH^- becomes complete above pH 7.

(3) Curve 5 shows the free [F⁻] calculated in a 2.5 × 10^{-3} M NaF solution between pH 2 and 8. In this range of pHs, we estimate the change in [F⁻] to be about 0.5 orders of magnitude, which corresponds to about 30 mV in the response of the F⁻ ISE. This amplitude of oscillations was predicted from curve 5 and was actually measured with the F⁻ ISE in the Al^{3+}-free, but F⁻-containing, BSM oscillator.

After examining the data obtained from the calculated [species] versus pH diagrams, we designed and carried out experiments in which the BSM pH oscillator was coupled to the equilibria represented by eqs 1−4. To the standard composition BSM oscillator (see Figure 2), we added a constant amount of [Al(NO$_3$)$_3$] = 6.25 × 10^{-4} M and increasing amounts of NaF to give [Al(NO$_3$)$_3$]/[NaF] ratios of 1:1, 1:2, 1:4, and 1:6. We monitored [F⁻] and pH simultaneously with the F⁻ ISE and a glass electrode, respectively. These amounts of Al(NO$_3$)$_3$ (mixed and introduced with the input $NaBrO_3$ solution) and NaF (mixed and introduced with the input Na_2SO_3) were found not to disturb the operation of the pH oscillator. The pH oscillated nearly as shown in Figure 2. The solution alternated between clear and cloudy states as the pH passed the break points on curves 1−4, Figure 5. The F⁻ ISE, as expected, showed oscillatory responses. The oscillatory traces recorded with the F⁻ ISE in the BSM oscillator at constant input [Al(NO$_3$)$_3$] and increasing [NaF] are presented in Figure 6. Figure 6 indicates that the largest changes in the signal of the F⁻ ISE (∼150 mV) were measured at [Al^{3+}]$_0$/[F⁻]$_0$ = 1:1 (part a). Under this condition, we predicted about 3 orders of magnitude change in [F⁻] from Figure 5, curve 1. As the ratio increases, the amplitude of oscillation decreases (parts b−d), as anticipated from the calculated lines shown in Figure 5, curves 2− 4.

We may summarize the [F⁻] oscillations observed in the BSM−Al(NO$_3$)$_3$−NaF flow system as follows. The BSM oscillator provides oscillations in the pH range between 2.5 and 7.2. At low pH, [F⁻] is low because the fluoride ions are complexed as $AlF_n^{(n-3)-}$. At high pH, the complex is converted to Al(OH)$_3$, the F⁻ ions are released, and [F⁻] becomes high. The robustness of the oscillations depends on the ratio of the input [Al(NO$_3$)$_3$] and [NaF].

Bistability in the BSM−Al(NO$_3$)$_3$−NaF System. Besides oscillations in pH, the BSM CSTR system can also show high- and low-pH steady states and hysteresis between them as one of the control parameters is varied.[5] We investigated whether a modified bistability, the existence of steady states of high and low [F⁻] under the same experimental conditions, may be generated if [Al(NO$_3$)$_3$] and [NaF] in 1:1 molar ratio are introduced into the bistable BSM system. The bistable domain in the BSM mixture can be reached from the oscillatory state by decreasing the input [BrO_3^-] and [Mn(II)]. The domain is largest when no input [Mn(II)] at all is used.[5] In order to shift the oscillatory BSM system shown in Figure 2 toward bistability, we halved the concentration of BrO_3^-, removed the Mn(II), and

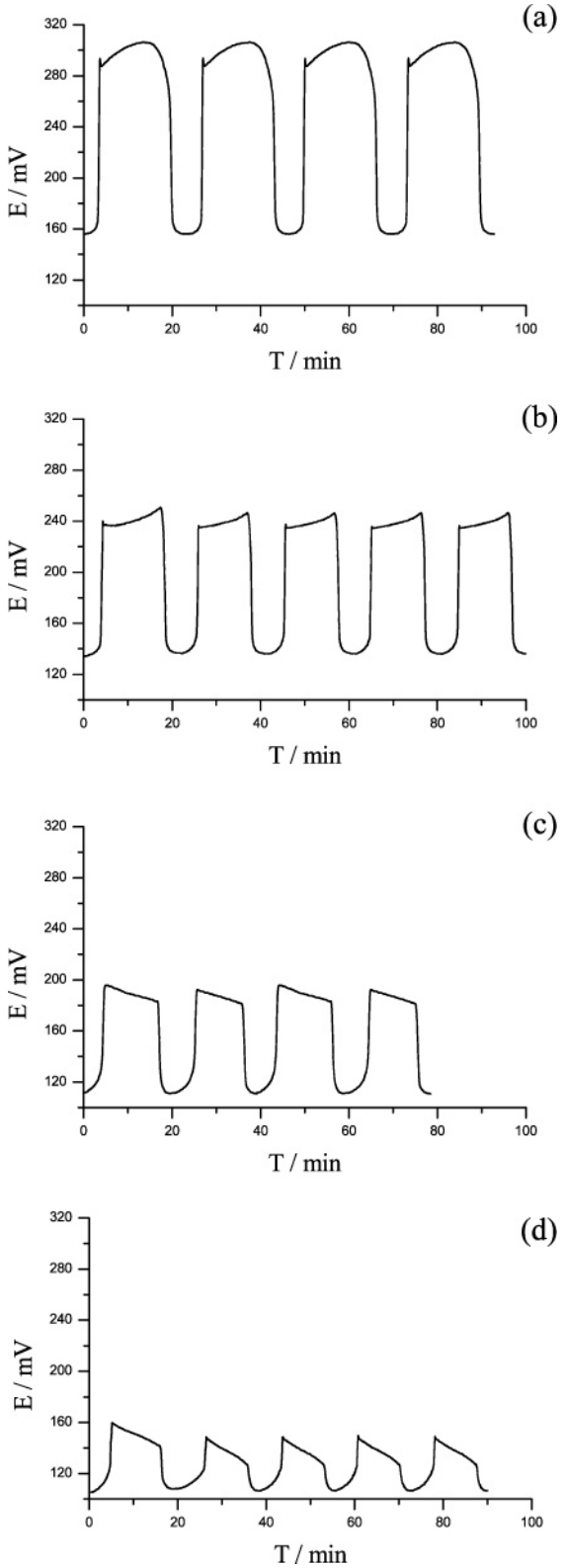

Figure 6. Oscillations in [F^-] measured with a F^- ISE in the BSM−$Al(NO_3)_3$−NaF flow systems. Parameters of the BSM pH oscillator are as those in Figure 2. Concentrations in the CSTR: (a) [$Al(NO_3)_3$] = 6.25×10^{-4} M and [NaF] = 6.25×10^{-4} M; (b) [$Al(NO_3)_3$] = 6.25×10^{-4} M and [NaF] = 1.25×10^{-3} M; (c) [$Al(NO_3)_3$] = 6.25×10^{-4} M and [NaF] = 2.5×10^{-3} M; (d) [$Al(NO_3)_3$] = 6.25×10^{-4} M and [NaF] = 3.75×10^{-3} M.

varied the flow rate, with all other parameters (input [Na_2SO_3], [$HClO_4$], temperature, stirring rate) unchanged. We measured the potentials of the F^- ISE and the glass electrode as a function of the flow rate (k_0) when the modified BSM system plus [$Al(NO_3)_3$] = [NaF] = 6.25×10^{-4} M were flowed into the CSTR. The results are shown in Figure 7. The high-pH steady state was maintained when the reactor was filled with the highest pump rate and the pump was kept running at high speed. Under this condition, the electrodes monitored a high-[F^-], high-pH (7.1) steady state (SSI). When we gradually decreased the flow rate, the potential of the electrodes changed only slightly until we reached $k_0 = 2 \times 10^{-3}$ s^{-1}, where a rapid transition to a low-[F^-], low-pH (∼2.6) steady state (SSII) occurred. When we varied the pump rate in the opposite direction, the system remained in this state until $k_0 = 5.5 \times 10^{-3}$ s^{-1}, where an abrupt transition back to SSI took place. Figure 7 demonstrates the existence of a wide hysteresis loop in the [F^-] versus flow rate plane. The difference in [F^-] between the SSI and SSII states is 2−3 orders of magnitude, in good agreement with that predicted from the distribution diagram in Figure 5, curve 1.

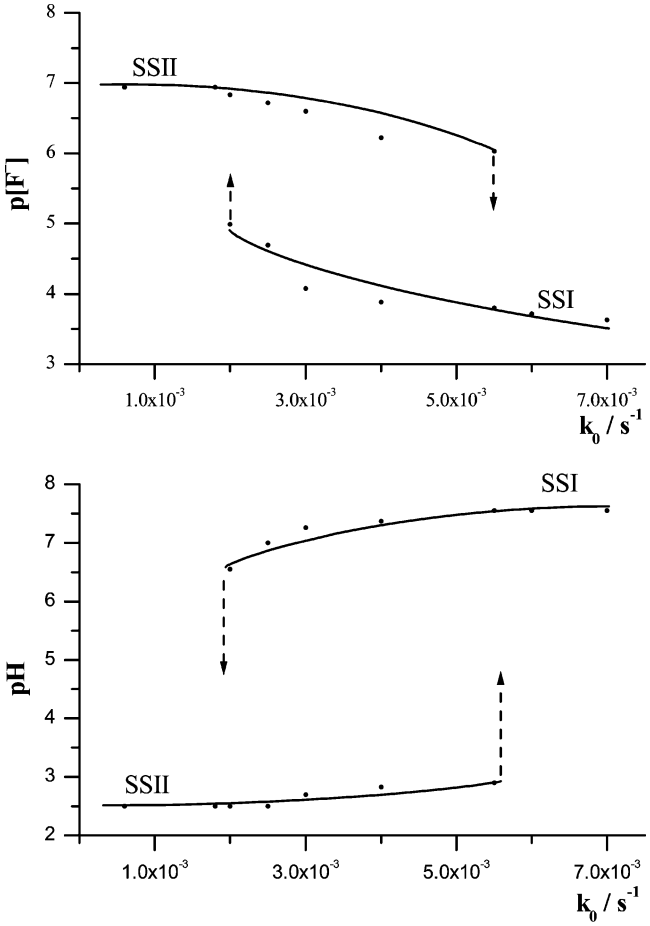

Figure 7. Hysteresis loops in the log[F^-] versus flow rate (k_0) and pH versus k_0 planes measured in the BSM−$Al(NO_3)_3$−NaF flow system. Parameters of the BSM oscillator are as those in Figure 2, except [$NaBrO_3$] = 7.5×10^{-4} M and [$MnSO_4$] = 0. [$Al(NO_3)_3$] = [NaF] = 6.25×10^{-4} M.

Oscillations in [F^-] in the BSM−CaEDTA−NaF System. Oscillations in [F^-] can also be observed in the BSM−CaEDTA−NaF system, but the amplitude of these oscillations is much smaller than that measured with Al^{3+} as the intermediary reagent between F^- and the core oscillator. Here, we generated the "Ca^{2+} oscillator" as described earlier,[2] but we used the BSM reaction instead of BSF for the primary oscillator to be coupled to the reaction in eq 2. The CaEDTA complex is stable at pH ≥ 6 but dissociates completely below pH 3. In the acid range of the pH oscillator, the free [Ca^{2+}] is equal to the initial [CaEDTA]. If we introduce F^- ions, CaF_2, a sparingly soluble precipitate, forms according to eq 4, and [F^-] decreases

below its value in the absence of precipitation. When the pH rises above 6, the EDTA drives F^- out of CaF_2, CaEDTA is reformed, and $[F^-]$ becomes high. We monitored the oscillations in the free $[F^-]$ with a F^- ISE, but the periodic appearance of the CaF_2 precipitate at the pH minimum and its dissolution in the high-pH region allowed us to follow the oscillations visually as well when $[CaEDTA] = 10^{-3}$ M and $[NaF] = 2 \times 10^{-3}$ M were used as inputs to the BSM system. The calculations predicted, and the experiments confirmed, that the amplitude of F^- oscillations in the BSM−CaEDTA−NaF reaction is much smaller than that in the BSM−$Al(NO_3)_3$−NaF system. The large difference in the amplitude is due to the large differences in the equilibrium constants. We present the F^- oscillations in the BSM−CaEDTA−NaF system here to demonstrate that either precipitation reactions like those of eq 1 or complexation equilibria as those in eq 2 can serve as the pH-dependent equilibrium in a multiply coupled system for inducing oscillations in the concentration of a nonredox species.

Conclusions

Our recent efforts in using oscillatory chemical reactions to drive chemical equilibria periodically between their initial and final states have resulted in a method which makes it possible to maintain high-amplitude oscillations in the concentration of ions that participate in the equilibrium process. In this way, periodic pulses in the concentrations of cations, anions, and even neutral molecules can be designed and produced experimentally. Earlier, we built "cation oscillators", in which oscillations in $[Al^{3+}]$ or $[Ca^{2+}]$ were induced.[2] In this work, we have shown that periodic pulses in the concentration of anions can also be generated if a second equilibrium is established in which an oscillatory cation and the target anion are involved. The chemistry in the second equilibrium follows the changes that occur in the first. If the product formed in the reaction between the cation and the anion is a stable complex or a precipitate, the periodic formation and decomposition of the undissociated product result in a low concentration of free anion when it is chemically bound. Its concentration then increases significantly when the anion is released from the complex or precipitate due to the effect of the core pH oscillator on the direction and the extent of the two consecutive equilibria.

The amplitude of the periodically induced ion pulses depends on the details of the equilibria, that is, on the conditional equilibrium constants at the minimum and the maximum pH of the core oscillator. The behavior at any pH during the oscillatory cycle can be estimated from equilibrium diagrams where the concentration distribution of all species as a function of pH is plotted. These diagrams—some of them shown in Figures 3−5—can be calculated with software like MEDUSA if the stoichiometry of the equilibria, the corresponding equilibrium constants, and the total concentrations of the initial reagents are known. Even if the calculations predict oscillations in the concentration of a given species, there remain several requirements for the successful creation of an oscillator. In particular, the constituents of the core oscillator must be compatible with those that participate in the equilibria; otherwise, the oscillator may be destroyed or the equilibrium may not go in the desired direction. The relative rates of the component processes must also be in appropriate ratios.

The approach of generating forced dynamical behavior in chemical systems is not restricted to oscillations. In addition to the induced bistability demonstrated in this paper, we note the recent stimulation of periodic switching between the folded and unfolded conformations of DNA,[7] driven by the IO_3^-−SO_3^{2-}−$S_2O_3^{2-}$ pH oscillator,[8] as a striking application of this concept.

Acknowledgment. This work was supported by the grants from the Hungarian Academy of Sciences (OTKA Nos K 67701 and K 62029), the U.S. National Science Foundation (NSF CHE-0615507), and a U.S.−Hungarian research grant from NSF and HAS. We thank Ariel Levy for assistance with some of the experiments.

Supporting Information Available: Distribution of species in mixtures containing $Al(NO_3)_3$ and NaF as a function of pH. This information is available free of charge via the Internet at http://pubs.acs.org.

References and Notes

(1) Kurin-Csörgei, K.; Epstein, I. R.; Orbán, M. *Nature* **2005**, *439*, 139−142.
(2) Kurin-Csörgei, K.; Epstein, I. R.; Orbán, M. *J. Phys. Chem. A* **2006**, *110*, 7588−7592.
(3) Rábai, G.; Orbán, M.; Epstein, I. R. *Acc. Chem. Res.* **1990**, *23*, 228−263.
(4) Edblom, E. C.; Luo, Y.; Orbán, M.; Kustin, K.; Epstein I. R. *J. Phys. Chem.* **1989**, *93*, 2722−2727.
(5) Okazaki, N.; Rábai, G.; Hanazaki, I. *J. Phys. Chem. A* **1999**, *103*, 10915−10920.
(6) Puigdomenech, I. *Chemical Equilibrium Software MEDUSA*, http://web.telia.com/~u156511596.
(7) Liedl, T.; Simmel, F. C. *Nano Lett.* **2005**, *5*, 1894−1898.
(8) Rábai, G.; Beck, M. T. *J. Phys. Chem.* **1988**, *92*, 2804−2807.